

Published in final edited form as:

*J Biomed Opt.* 2009 ; 14(4): 040507. doi:10.1117/1.3207156.

## Complementary optical and nuclear imaging of caspase-3 activity using combined activatable and radiolabeled multimodality molecular probe

Hyeran Lee<sup>a</sup>, Walter J. Akers<sup>a</sup>, Philip P. Cheney<sup>a</sup>, W. Barry Edwards<sup>a</sup>, Kexian Liang<sup>a</sup>, Joseph P. Culver<sup>a</sup>, and Samuel Achilefu<sup>a,b,\*</sup>

<sup>a</sup> Department of Radiology, Washington University School of Medicine, St. Louis, MO 63110

<sup>b</sup> Department of Biochemistry & Molecular Biophysics, Washington University School of Medicine, St. Louis, MO 63110

### Abstract

Based on the capability of modulating fluorescence intensity by specific molecular events, we have developed a new multimodal optical-nuclear molecular probe with complementary reporting strategies. The molecular probe (LS498) consists of DOTA for chelating a radionuclide, a near infrared fluorescent dye, and an efficient quencher dye. The two dyes were separated by a cleavable peptide substrate for caspase-3, a diagnostic enzyme that is upregulated in dying cells. LS498 was radiolabeled with <sup>64</sup>Cu, a radionuclide used in positron emission tomography. In the native form, LS498 fluorescence was quenched until caspase-3 cleavage of the peptide substrate. Enzyme kinetics assay showed that LS498 was readily cleaved by caspase-3, with excellent enzyme kinetic parameters  $k_{cat}$  and  $K_M$  of  $0.55 \pm 0.01 \text{ s}^{-1}$  and  $1.12 \pm 0.06 \text{ }\mu\text{M}$ , respectively. In mice, the initial fluorescence of LS498 was 10-fold less than control. Using radiolabeled <sup>64</sup>Cu-LS498 in a controlled and localized *in vivo* model of caspase-3 activation, a time-dependent 5-fold NIR fluorescence enhancement was observed but radioactivity was the same in caspase-3 positive and negative controls. These results demonstrate the feasibility of using radionuclide imaging for localizing and quantifying the distribution of molecular probes and optical imaging for reporting the functional status of diagnostic enzymes.

### Keywords

optical imaging; nuclear imaging; scintigraphy; caspase-3; NIR FRET

### 1 Introduction

Multimodal imaging has been driven by the realization that no single imaging method has complete solution to the multifaceted challenges of disease diagnosis and prognosis. For example, the addition of molecular imaging to the current functional and structural imaging methods requires procedures that report molecular events without loss of anatomical information. A common practice today is to combine methods with high spatial resolution such as magnetic resonance imaging (MRI), X-ray computed tomography (CT), and ultrasound with those with high detection sensitivity such as positron emission tomography

Address correspondence to: Samuel Achilefu, Ph.D., Department of Radiology, 4525 Scott Ave. Saint Louis, MO 63110, Telephone: 314-362-8599, Fax: 314-747-5191, achilefu@mir.wustl.edu.

(PET) and diffuse optical tomography (DOT). For optical imaging, explicitly incorporating a priori anatomical knowledge into light modeling and image reconstruction.<sup>1-3</sup>

A less utilized multimodal strategy is the combination of two functional or molecular imaging methods, such as optical-nuclear multimodal imaging. As summarized in a recent report, there are many reasons to utilize this hybrid of two modalities with similarly high detection sensitivity.<sup>4</sup> For example, although combining molecular optical contrasts with MRI or CT provides co-registered reference anatomy, the disparate contrast mechanisms present a barrier to integrating the imaging data. Because of the high sensitivity of both PET and optical methods and the compatibility of their imaging agents, we and others have reported the use of monomolecular multimodality imaging agents (MOMIAs) for combined nuclear-optical imaging studies.<sup>5-7</sup> These studies have established the equivalence or identical origin of signals from both contrast sources through image co-registration. The dual optical-nuclear imaging approach has been extended to nanomaterials, where PET and optical imaging has been combined to improve quantitative accuracy.<sup>8, 9</sup>

In this study, we sought to develop a complementary imaging strategy that would harness the strengths of NIR fluorescence and nuclear imaging methods. To achieve this goal, we hypothesized that incorporating activatable fluorescent molecular system into a radiolabeled cleavable peptide will provide a unique opportunity to fuse imaging data with identical pharmacokinetics but different reporting strategies. Accordingly, we prepared a multifunctional molecular probe (LS498) with persistent radionuclide signal and activatable fluorescence in response to a specific molecular process.

## 2 Methods

The peptide backbone, metal chelating group DOTA, and NIR fluorescent dye<sup>10</sup> used in LS498 (Fig. 1) were assembled as described previously.<sup>11</sup> The NIR fluorescent quencher, IR dye QC-1 (LICOR, NE) was incorporated into the multifunctional peptide at room temperature in PBS for 24 h. The purified LS498 (5 $\mu$ g, 1.3 nmol) was radioabeled by heating (60 °C, 0.5 h) with <sup>64</sup>Cu (470  $\mu$ Ci) in aqueous buffer (100 mM NH<sub>4</sub>OAc, pH 5.5). The caspase-3 enzyme kinetic parameters  $k_{cat}$  and  $K_M$  were determined by incubating LS498 (0.27 to 35  $\mu$ M) with caspase-3 (290 pM) in assay buffer. The fluorescence released by enzyme-mediated hydrolysis was measured at multiple time points on a Biotek Synergy HT plate reader ( $\lambda_{EX}$ =760/40 nm,  $\lambda_{EM}$ =810/40 nm). The data generated was analyzed as previously described.<sup>12</sup>

As a model of tumor-related caspase activity, plastic tubes containing <sup>64</sup>Cu-LS498 (50  $\mu$ L; 1  $\mu$ M) and either 260 pM caspase-3 or 5  $\mu$ M BSA in assay buffer were implanted subcutaneously in opposite flanks of the mouse. Multimodal imaging and region of interest (ROI) analysis of fluorescence (755 nm excitation, 830 nm emission), X-ray, and scintigraphy were performed with the IS4000MM (Carestream Health, New Haven, CT) as previously described.<sup>5</sup>

## 3 Results and Discussion

### 3.1 Development of caspase-3 activatable probe for dual optical-nuclear imaging

A multifunctional peptide-based molecular probe LS498 (Fig. 1) was designed and prepared for use in this study. Because of the need to monitor the response of diseased tissue to treatment and the implication of caspase-3 in early cell death,<sup>12</sup> LS498 was specifically developed to report the activity of this diagnostic enzyme. To accomplish this goal, we used a FRET system, where the fluorescence of a NIR dye was efficiently quenched with wide-spectrum quencher dye. Since the tetrapeptide sequence, Aspartic acid-Glutamic-acid-

Valine-Aspartic acid (DEVD), is an established substrate for caspases-3,<sup>12</sup> we incorporated this peptide sequence between the two dyes. Cleavage of the DEVD peptide results in fluorescence enhancement that can be used to monitor the enzyme activity.<sup>12, 13</sup> In the quenched state, it is not feasible to image the distribution of the molecular probe in tissue prior to enzyme cleavage. Moreover, lack of fluorescence enhancement may be due to inadequate delivery of the molecular probe to the target tissue, a situation that could result in false-negative outcomes. To address this issue, LS498 was labeled with <sup>64</sup>Cu, a positron emitter with half-life of 12.8 h. This radionuclide is widely used in PET imaging of molecular processes in small animals and humans.<sup>14</sup> After HPLC purification, LS498 was labeled with <sup>64</sup>Cu at high specific activity (360 Ci/mmol) and purity (>99%). In previous work with <sup>64</sup>Cu-DOTA-c(RGDyK), specific activities ranged from 200–500 Ci/mmol and receptor specific tumor accumulation allowed for  $\alpha_v\beta_3$ -positive tumor visualization by small animal PET.<sup>15</sup> Therefore, the observed specific activity in LS498 is adequate for receptor targeted tumor imaging in vivo.

### 3.2 Caspase-3 Enzyme Kinetics

The feasibility of applying a reporter of proteolytic activity to in vivo imaging depends on how fast the substrate is processed by the enzyme before being washed away from the target site. The kinetic parameters,  $k_{cat}$  and  $K_M$ , are measurable indicators of how well a substrate is processed by an enzyme. Our study shows that LS498 was readily cleaved by caspase-3 and displayed classic Michaelis-Menten kinetics (Fig. 2) with enzyme kinetic parameters  $k_{cat}$  and  $K_M$  of  $0.55 \pm 0.01 \text{ s}^{-1}$  and  $1.12 \pm 0.06 \text{ }\mu\text{M}$ , respectively. The observed  $k_{cat}$  and  $K_M$  compares favorably with standard substrates Ac-DEVD-AMC ( $k_{cat} = 0.75 \text{ s}^{-1}$ ,  $K_M = 9.7 \text{ }\mu\text{M}$ ) and Ac-DEVD-pNA ( $k_{cat} = 0.55 \pm 0.01 \text{ s}^{-1}$ ,  $K_M = 11 \text{ }\mu\text{M}$ ). The  $k_{cat}/K_M$  ratio, which measures the performance constant of an enzyme for a substrate, was found to be  $4.91 \times 10^5 \text{ s}^{-1} \text{ M}^{-1}$ .

### 3.3 In vivo imaging of LS-498 distribution and model of caspase-3 activation

LS498 was designed to prevent fluorescence emission prior to activation by caspase-3. To assess if this goal was met, we compared the fluorescence emission of LS498 to a control analogue. The control peptide lacks a quencher dye, thereby reported the maximum fluorescence intensity of a completely cleaved LS498. Intravenous injection of the two molecular probes in healthy mice showed that fluorescence was hardly detectable in the mouse injected with LS498 and remained lower than that of the control probe up to 24 h post-injection. Immediately after injection (30 minutes), the fluorescence intensity was at least 10-fold less for LS498 relative to control (Fig. 3A). After 24 h, both molecular probes had similar low fluorescence intensity (data not shown), approaching the detection limit of our imaging system. Interestingly, the kidneys were visible at 24 h in both mice, suggesting a possible degradation of LS498 after prolonged retention in this organ. Alternatively, it is also possible that the kidneys express residual levels of caspase-3 that was responsible for the observed fluorescence enhancement.

To evaluate the feasibility of imaging caspase-3 activity in small animals, we developed an artificial model of subcutaneous tumor in mice. Two tubes containing radiolabeled <sup>64</sup>Cu-LS498 were each mixed with either caspase-3 or bovine serum albumin (BSA) to mimic tissues expressing caspase-3 versus control, respectively. Expectedly, the fluorescence of caspase-3 containing tube increased with time, reaching a plateau after 4 h. In contrast, the BSA control tube did not show any fluorescence enhancement up to 24 h (Fig. 3B). In contrast to the scintigraphy image where both tubes had similar radioactivity, the optical imaging clearly distinguished caspase-3 positive from the negative tube based on differences in their fluorescence intensity. These findings demonstrate the feasibility of using LS498 to report concentration through nuclear contrast and enzyme activity through optical contrast in

a controlled in vivo context. To be effective in a tumor model, LS498 has to be internalized in cells where the cytosolic caspase-3 resides. Cytosolic delivery could be achieved by incorporating cell-permeating peptides to LS498 or via receptor-mediated endocytosis mechanism that is coupled with endosomal disrupting peptides.

In conclusion, this paper summarizes our ongoing efforts toward the development of multimodality imaging agents for combined optical and nuclear molecular imaging of diseased tissues. In this study, the always “on” nuclear signal is useful for quantifying and localizing the distribution of the probe while the optical imaging will report the functional status of a target molecular event. Both in vitro and in vivo results demonstrate the feasibility of using this approach to image molecular processes. Although we used caspase-3 as a model for this study, the complementary contrast strategy is applicable to imaging the functional status of most enzymes. Studies are in progress to demonstrate the utility of this new imaging strategy in animal disease models.

## Acknowledgments

We thank LICOR for the generous gift of the quencher dye used in this study. This study was funded in part by the National Institutes of Health (R01 CA109754 and R01EB008458).

## References

1. Barbour RL, Graber HL, Chang J, Barbour SS, Koo PC, Aronson R. MRI-guided optical tomography: prospects and computation for a new imaging method. *IEEE Comput Sci Eng* 1995;2:63–77.
2. Barnett AH, Culver JP, Sorensen AG, Dale A, Boas DA. Robust inference of baseline optical properties of the human head with three-dimensional segmentation from magnetic resonance imaging. *Appl Optics* 2003;42:3095–3108.
3. Pogue BW, Paulsen KD. High-resolution near-infrared tomographic imaging simulations of the rat cranium by use of apriori magnetic resonance imaging structural information. *Opt Lett* 1998;23:1716–1718. [PubMed: 18091894]
4. Culver J, Akers W, Achilefu S. Multimodality molecular imaging with combined optical and SPECT/PET modalities. *J Nucl Med* 2008;49:169–172. [PubMed: 18199608]
5. Edwards WB, Akers WJ, Ye Y, Cheney PP, Bloch S, Xu B, Laforest R, Achilefu S. Multimodal Imaging of Integrin Receptor-Positive Tumors by Bioluminescence, Fluorescence, Gamma Scintigraphy, and Single-Photon Emission Computed Tomography Using a Cyclic RGD Peptide Labeled with a Near-Infrared Fluorescent Dye and a Radionuclide. *Mol Imaging* 2009;8:101–110. [PubMed: 19397855]
6. Li C, Wang W, Wu Q, Ke S, Houston J, Sevic-Muraca E, Dong L, Chow D, Charnsangavej C, Gelovani JG. Dual optical and nuclear imaging in human melanoma xenografts using a single targeted imaging probe. *Nucl Med Biol* 2006;33:349–358. [PubMed: 16631083]
7. Zhang Z, Liang K, Bloch S, Berezin M, Achilefu S. Monomolecular multimodal fluorescence-radioisotope imaging agents. *Bioconjug Chem* 2005;16:1232–1239. [PubMed: 16173803]
8. Cai W, Chen K, Li ZB, Gambhir SS, Chen X. Dual-function probe for PET and near-infrared fluorescence imaging of tumor vasculature. *J Nucl Med* 2007;48:1862–1870. [PubMed: 17942800]
9. Duconge F, Pons T, Pestourie C, Herin L, Theze B, Gombert K, Mahler B, Hinnen F, Kuhnast B, Dolle F, Dubertret B, Tavitian B. Fluorine-18-labeled phospholipid quantum dot micelles for in vivo multimodal imaging from whole body to cellular scales. *Bioconjug Chem* 2008;19:1921–1926. [PubMed: 18754572]
10. Lee H, Berezin MY, Henary M, Streckowski L, Achilefu S. Fluorescence lifetime properties of near-infrared cyanine dyes in relation to their structures. *J Photochem Photobiol A-Chem* 2008;200:438–444. [PubMed: 20016664]
11. Achilefu S, Jimenez HN, Dorshow RB, Bugaj JE, Webb EG, Wilhelm RR, Rajagopalan R, Johler J, Erion JL. Synthesis, in vitro receptor binding, and in vivo evaluation of fluorescein and

- carbocyanine peptide-based optical contrast agents. *J Med Chem* 2002;45:2003–2015. [PubMed: 11985468]
12. Bullok KE, Maxwell D, Kesarwala AH, Gammon S, Prior JL, Snow M, Stanley S, Piwnica-Worms D. Biochemical and in vivo characterization of a small, membrane-permeant, caspase-activatable far-red fluorescent peptide for imaging apoptosis. *Biochem* 2007;46:4055–4065. [PubMed: 17348687]
  13. Zhang Z, Fan J, Cheney PP, Berezin MY, Edwards WB, Akers WJ, Shen D, Liang K, Culver JP, Achilefu S. Activatable Molecular Systems Using Homologous Near-Infrared Fluorescent Probes for Monitoring Enzyme Activities in Vitro, in Cellulo, and in Vivo. *Mol Pharm.* 2009
  14. Lewis MR, Wang M, Axworthy DB, Theodore LJ, Mallet RW, Fritzberg AR, Welch MJ, Anderson CJ. In vivo evaluation of pretargeted <sup>64</sup>Cu for tumor imaging and therapy. *J Nucl Med* 2003;44:1284–1292. [PubMed: 12902420]
  15. Chen X, Park R, Tohme M, Shahinian AH, Bading JR, Conti PS. MicroPET and autoradiographic imaging of breast cancer alpha v-integrin expression using <sup>18</sup>F- and <sup>64</sup>Cu-labeled RGD peptide. *Bioconjug Chem* 2004;15:41–49. [PubMed: 14733582]

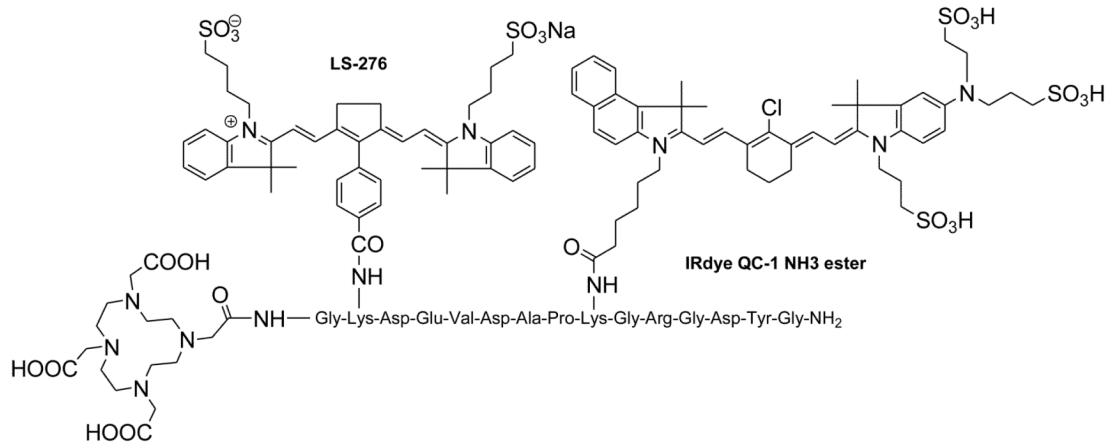


**Fig. 1.**  
Structure of caspase-3 activatable optical-nuclear molecular probe (LS498)

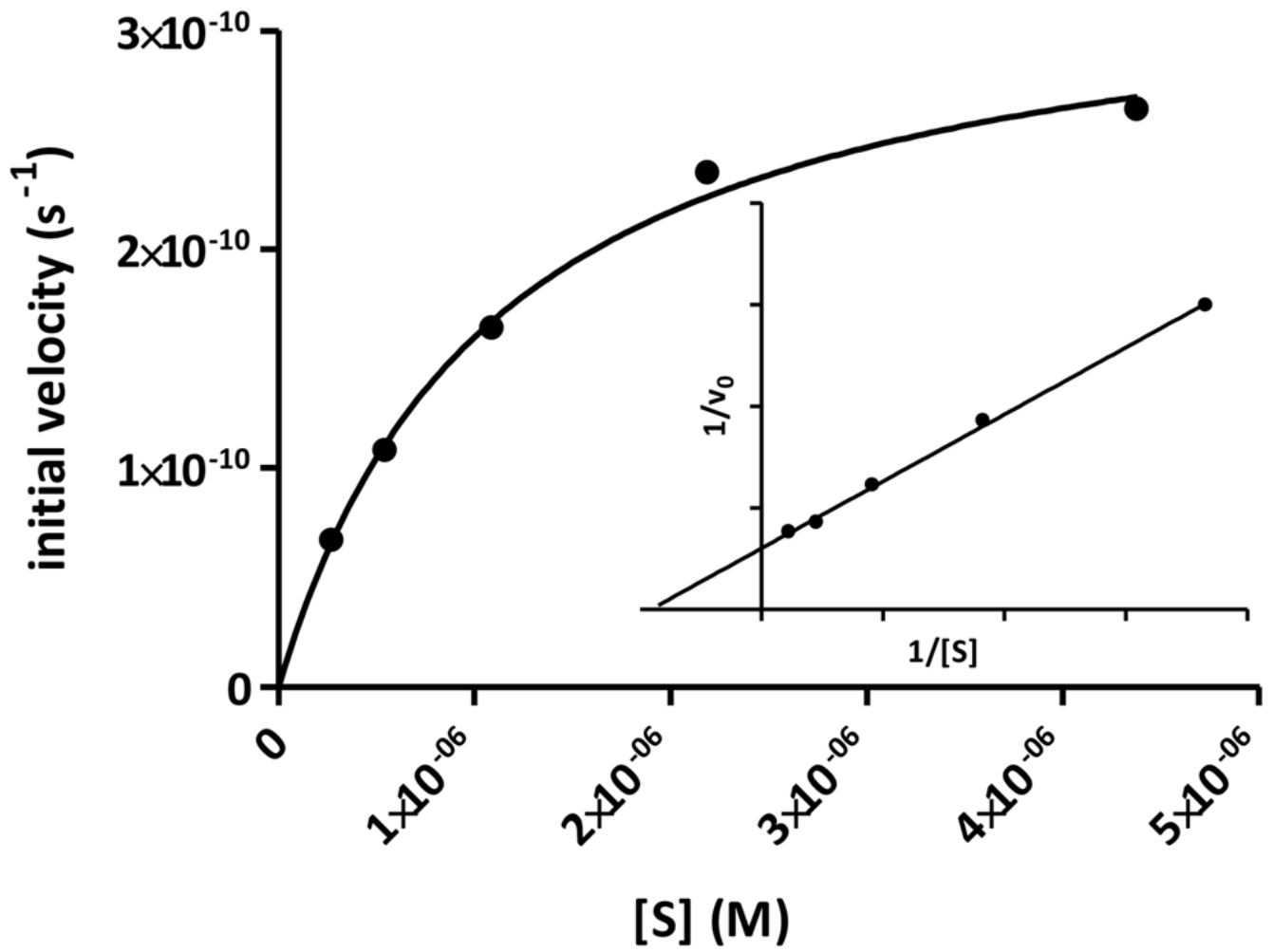
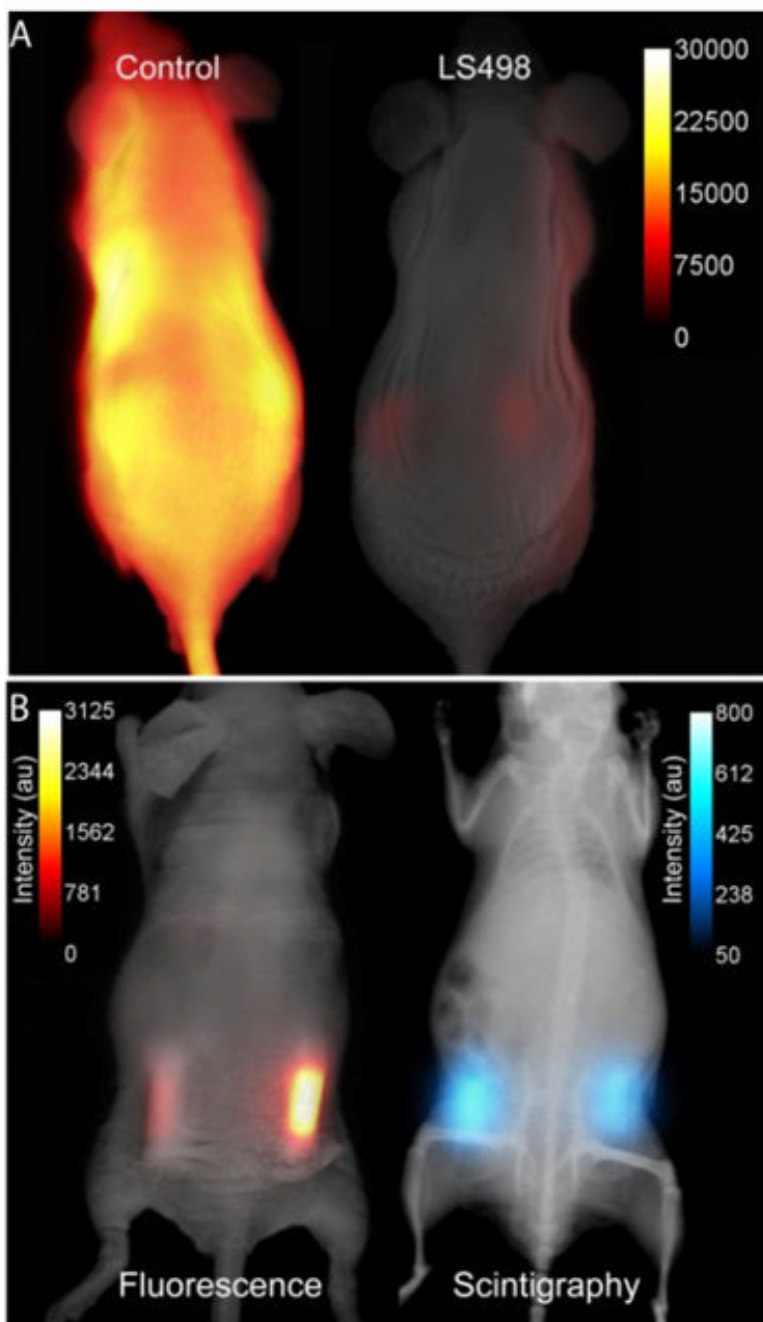


Fig. 2. Nonlinear fit of initial velocity with respect to substrate concentration and the corresponding Lineweaver-Burk plot (insert). Substrate concentrations varied from 270 nM to 35  $\mu\text{M}$ .





**Fig. 3.** Imaging of multifunctional molecular probe in mice. (A) In vivo distribution of LS498 (Right) and non-quenched control analogue (Left) in mice at 30 minutes after intravenous injection of the imaging agents. Fluorescence of the activatable probe was efficiently quenched by greater than 16-fold relative to the non-quenched control. (B) Multimodal fluorescence (Left) and scintigraphic (Right) imaging of a mouse with subcutaneously implanted tubes containing  $^{64}\text{Cu}$ -LS498 with BSA (left side) or caspase-3 (right side) 2 h after implantation. Tubes were implanted subcutaneously (about 1 mm) below the surface of the skin. Radioactivity is always “on” but fluorescence enhancement depends on the presence of caspase-3. The ratio of fluorescence intensity for the caspase-3 sample was 4.2



times greater than the control sample and this ratio increased to 5.6-fold after normalizing to radioactivity.